



# Adipose-derived exosomes deliver miR-23a/b to regulate tumor growth in hepatocellular cancer by targeting the VHL/HIF axis

Yang Liu<sup>1</sup> · Juan Tan<sup>1</sup> · Shuangyan Ou<sup>2</sup> · Jun Chen<sup>3</sup> · Limin Chen<sup>1</sup> 

Received: 10 January 2019 / Accepted: 26 June 2019 / Published online: 18 July 2019  
© University of Navarra 2019

## Abstract

Adipose tissue has long been considered to be involved in tumor progression. However, the adipocyte-secreted molecular determinants that regulate hepatocellular cancer progression have not been defined yet. In this study, the expression pattern of exosome miRNAs in hepatocellular carcinoma (HCC) patients with high body fat ratio (BFR) were identified by using low-density microarray. And the targets of exosome-miRNAs in HCC cells were predicted by bioinformatics methods and verified by in vitro as well as in vivo experiments. Here, we show that microRNA-23a/b (miR-23a/b) was significantly upregulated in both serum exosomes and tumor tissues of HCC patients with a high body fat ratio than low BFR. Subsequently, in vitro studies suggested that miR-23a/b was most likely to be derived from adipocytes and was transported into cancer cells via exosomes, thus promoting HCC cell growth and migration. Meanwhile, exosome miR-23a and miR-23b confer chemoresistance by targeting the von Hippel-Lindau/hypoxia-inducible factor axis. Our study provides evidence in that high BFR-related exosome miR23-a/b is a promising target for future treatment of HCC.

**Keywords** Adipose · Exosomes · miR-23 · HIF · HCC

## Introduction

Overweight and obesity have been demonstrated to be important carcinogenic risk factors, leading to a significant increase in HCC risk [10]. Epidemiological studies

have established that obesity has become a serious threat to public health worldwide, leading to a number of public health problems, such as the increased risk of liver cancer [2, 17]. However, the direct molecular mechanism that obesity and adipose promote occurrence and development of HCC is still far from being fully understood.

Recent studies have shown a vital component of the tumor microenvironment in addition to initiation via soluble mediators; cell-cell communication can be initiated via surface interactions between circulating exosomes and trans-membrane molecules expressed by target cells [16].

It is interesting that exosomes could transfer miRNA, which are extremely stable and participated in lots of physiological and pathological processes, such as cell differentiation, proliferation, apoptosis, and tumor genesis [3, 13]. As reported, miR-23 acted as a common oncogene, which could promote progression of cancer [1, 12]. It has also been reported that miR-23a could regulate the metabolism in tumorigenesis, such as suppression of miR-23a/b which could enhance glutamine metabolism in prostate cancer [4]. Recent study has shown that miR-23b inhibition has an anti-proliferation effect on HCC [9].

Hypoxia-inducible factor 1 $\alpha$  (HIF-1 $\alpha$ ) is a key transcription factor of oxygen homeostasis regulation [11]. The expression of HIF-1 $\alpha$  is regulated through

---

✉ Limin Chen  
chenliminxymc@163.com

Yang Liu  
liuyangxymc@163.com

Juan Tan  
tanjuanxymc@163.com

Shuangyan Ou  
oushuangyan@163.com

Jun Chen  
chenjunxymc@163.com

<sup>1</sup> Department of Pathology, Infectious Diseases Institute, The Third Xiangya Hospital of Central South University, Changsha, Hunan, China

<sup>2</sup> Medical Oncology Institute, Hunan Cancer Hospital, Changsha, Hunan, China

<sup>3</sup> Hunan Polytechnic of Environment and Biology, Hengyang, Hunan, China

ubiquitin-mediated proteolysis, and is governed by the activity of Von Hippel-Lindau (VHL), which is known as a tumor suppressor [8]. VHL syndrome, an inherited familial syndrome related to cancer, is characterized by a predisposition to develop various types of tumors, including clear cell renal carcinomas, retinal and central nervous system hemangioblastomas, pheochromocytomas, and endolymphatic sac tumors [5, 7, 19].

In this study, we identified miR-23a/b in exosomes secreted from adipocytes. We demonstrated that exosomes deliver miR-23a/b from adipocytes to HCC cells, and we identified that VHL/HIF-1 $\alpha$  was targeted by miR-23a/b to modulate the ability of HCC cells, including proliferation, metastasis, and chemoresistance to 5-Fu.

## Materials and methods

### Human samples

Human tumor tissues from obese and non-obese patients were obtained from the Third Xiangya Hospital. The collection of human samples was approved by the local Ethical Committee and the Review Board of the Third Xiangya Hospital of Central South University. All the participants were informed of the usage of the samples, and consent forms were obtained.

### Animal studies

C57BL/6J male mice were purchased from the Model Animal Research Center of Nanjing University (Nanjing, China). All of the experimental procedures were performed in accordance with protocols approved by the Institutional Animal Care and Research Advisory Committee of Central South University. A lentiviral expression plasmid that can express miR-23a/b was purchased from GenePharma (Shanghai, China). Hepa 1–6 cells were infected with a control lentivirus or a miR-23a/b lentivirus. After transfecting the lentivirus, SW480 cells were subcutaneously injected into the mouse model ( $3 \times 10^6$  cells in 0.2 mL PBS per mouse, 5 mice per group). Mice were sacrificed 28 days after injection to remove the xenografted tumors, and the weights of the tumors were measured. A portion of the tissues was used for protein and total RNA extraction.

### Cell lines and culture conditions

BEL-7402, BEL-7402/5-Fu, Hepa1–6, and 3T3-L1 cells were bought from the cell bank of the Chinese Academy of

Sciences (Shanghai, China). BEL-7402, BEL-7402/5-Fu, and Hepa1–6 were maintained in DMEM medium supplemented with 10% FBS and penicillin/streptomycin (Life Technologies Corp., Grand Island, NY, USA). The 3T3-L1 cells were cultured in low-glucose DMEM media containing 10% FBS.

### Pre-adipocyte differentiation

The cells were induced to differentiate by culturing them for 2 days in an induction medium consisting of DMEM supplemented with 10% fetal bovine serum and 850 nM insulin (Sigma-Aldrich #I1882), 0.5  $\mu$ M dexamethasone (Sigma-Aldrich #D4902), 250  $\mu$ M 3-isobutyl-1-methylxanthine (IBMX, Sigma-Aldrich #I5879), 1  $\mu$ M rosiglitazone (Cayman Chemical #71742), 1 nM 3,3,5-triiodo-L-thyronine (T3, VWR #100567-778), and 125 nM indomethacin (Sigma-Aldrich #I7378). Subsequently, after 2 days the induction medium was replaced with DMEM supplemented with 10% FBS and 160 nM insulin and 1 nM T3 for another 2 days. The cells were then cultured in DMEM 10% FBS and 1 nM T3 until day 8 of differentiation, and the medium was replaced every other day. Oil Red O staining (Sigma-Aldrich) and triglyceride measurements of both mature adipocytes during differentiation were performed following the manufacturer's instructions to determine adiposity.

### Western blot analysis

Cell extracts were prepared in RIPA buffer (Beyotime, Shanghai, China) containing a complete protease inhibitor mixture (Beyotime, Shanghai, China). Proteins were separated on SDS-PAGE (Bio-Rad). The primary antibodies were used for western blotting: anti-CD63 (ab216130), anti-TSG101 (ab125011), anti-Alix (ab117600), anti-CD9 (ab92726), anti-VHL (ab77262), anti-HIF-1 $\alpha$  (ab187524), anti- $\alpha$ -tubulin (ab15246), and anti-GLUT-1 (ab32551) antibodies were purchased from Abcam (Cambridge, MA, USA).

### Exosome isolation from medium and serum

Exosomes were isolated from the cell culture medium by differential centrifugation, according to previous publications [20]. After removing cells and other debris by centrifugation at 300g and 3000g, the supernatant was centrifuged at 10,000g for 30 min to remove shedding vesicles and the other vesicles with bigger sizes. Finally, the supernatant was centrifuged at 110,000g for 70 min (all steps were performed at 4  $^{\circ}$ C); exosomes were collected

from the pellet and re-suspended in PBS. Serum exosomes were isolated by using an exosome isolation kit (Thermo), following the manufacturer's instruction.

### Electron microscopy

For electron microscopy observation, exosome pellets were fixed in 4% paraformaldehyde at 4 °C for 1 h. Then, the pellets were loaded onto electron microscopy grids coated with Formvar carbon, contrasted, and embedded in a mixture of uranyl acetate and methylcellulose. Sections were observed with a Philips Tecnai 10 transmission electron microscope operating at 80 kV (Phillips Electronic Instruments, Mathway, NJ, USA).

### Quantitative real-time PCR

Total RNA was extracted from cultured cells, tissue samples, or purified exosomes using TRIzol Reagent (Invitrogen, CA, USA). To quantify mature miR-23a/b, TaqMan Probes were used according to the manufacturer's instructions. U6 snRNA was used as an internal control, and the relative amount of miRNA normalized to U6 was calculated with the equation  $2^{-\Delta\Delta CT}$  in which  $\Delta\Delta CT = (CT_{miR-23a/b} - CT_{U6})_{tumor} - (CT_{miR-23a/b} - CT_{U6})_{control}$ .

For the mRNA expression analysis, oligo(dT)18 primers (TaKaRa) were used to reverse transcribe total RNA into cDNA. Then, a qRT-PCR was run by using SYBR Green dye (Invitrogen) and specific primers for VHL and GAPDH. The primer sequences were as follows: VHL (sense): GGGAACGGGGTGGGTTTAG; VHL (antisense): GCTCGCGTGAGTTCACAGA;  $\alpha$ -tubulin (sense): CGAGCCACATCGCTCAGACA; and  $\alpha$ -tubulin (antisense): GTGGTGAAGACGCCAG.

### CCK-8 assay

BEL-7402 and BEL-7402/5-Fu cells were seeded in a 96-well plate and then co-cultured with 3T3-exo for 24 h. After 48 h of 5-Fu treatment, the cell proliferation index was measured using a Cell Counting Kit-8 (CK04-500, Dojindo, Japan) according to the manufacturer's instruction. Absorbance was measured at a wavelength of 450 nm.

### Cell migration assay

Cell migration assays were performed using Millipore 24-well plates containing an 8- $\mu$ m pore membrane. Cells were harvested 24 h after co-culture with exosomes and suspended in FBS-free DMEM culture medium. The cells were then added

to the upper chamber ( $2 \times 10^4$  cells/well), and 0.5 mL DMEM plus 20% FBS was added to the lower compartment. The transwell-containing plates were incubated for 24 h in the incubator. After incubation, cells that had migrated to the lower surface of the filter membrane were fixed with 4% paraformaldehyde for 25 min at room temperature. The lower surfaces (with migrating cells) were captured by photomicroscopy (BX51 Olympus, Japan), and the cells were counted blindly (five fields per chamber).

### EdU assay

BEL-7402 cells were seeded in 48-well plates (Corning). After co-culture with exosomes, when the confluency of SW480 cells reached 80%, an EdU assay kit (RiboBio, Guangzhou, China) was used to determine the proliferation rate of the cells, following the manufacturer's instruction.

### Immunohistochemical analysis

Immunolocalization of VHL was performed using the tumor sections obtained from hepatocellular cancer patients. Slides containing the sections were stained with commercially available anti-VHL (1:500; ab77262) antibodies from Abcam. Target protein expression was visualized using a Betazoid 3,3'-diaminobenzidine chromogen kit (Biocare Medical, Concord, CA, USA).

### Luciferase reporter gene activity assay

BEL-7402 cells were seeded in 24-well plates 1 day before transfection. The cells were transfected with 0.2  $\mu$ g of the VHL reporter construct containing the predicted miR23a/b-binding sites, together with 0.2  $\mu$ g of  $\beta$ -galactosidase ( $\beta$ -gal) expression plasmid (Ambion), and equal amounts (50 pmol) of miR-23a/b mimic, miR-23a/b inhibitor, or the scrambled negative control RNAs using Lipofectamine 2000 (Invitrogen). The cells were treated using a luciferase assay kit 24 h post-transfection (Promega, Madison, WI, USA).

### Statistical analysis

All data were representative of five or six independent experiments. Data were expressed as mean  $\pm$  s.e. of at least five separate experiments. Statistical significance was considered at  $P < 0.05$  using the Student *t* test. In this study,  $*P < 0.05$ ,  $**P < 0.01$ , and  $***P < 0.001$ .

## Results

### Exosome miR-23a/b are upregulated in HCC patients with high BFR

Firstly, serum exosomes of HCC patients were isolated and identified. We characterized and quantified the serum exosomes by electron microscopy (Fig. 1a), western blot analysis (Fig. 1b), and nanoparticle tracking analysis (NTA) (Fig.

1c). According to the mean number of BFR, we divided HCC patients into BFR-high group and BFR-low group (Fig. 1d). miR-23 is a vital oncogene in HCC progression; thus, we detected serum exo-miR-23 level, which showed a positive correlation with BFR (Fig. 1e). VHL protein, which is a tumor suppressor, can directly mediate the ubiquitylation and proteasomal degradation of HIF-1 $\alpha$  to maintain HCC progression. VHL was negatively correlated, while HIF-1 $\alpha$  was positively correlated with BFR (Fig. 1f and g). However, the VHL

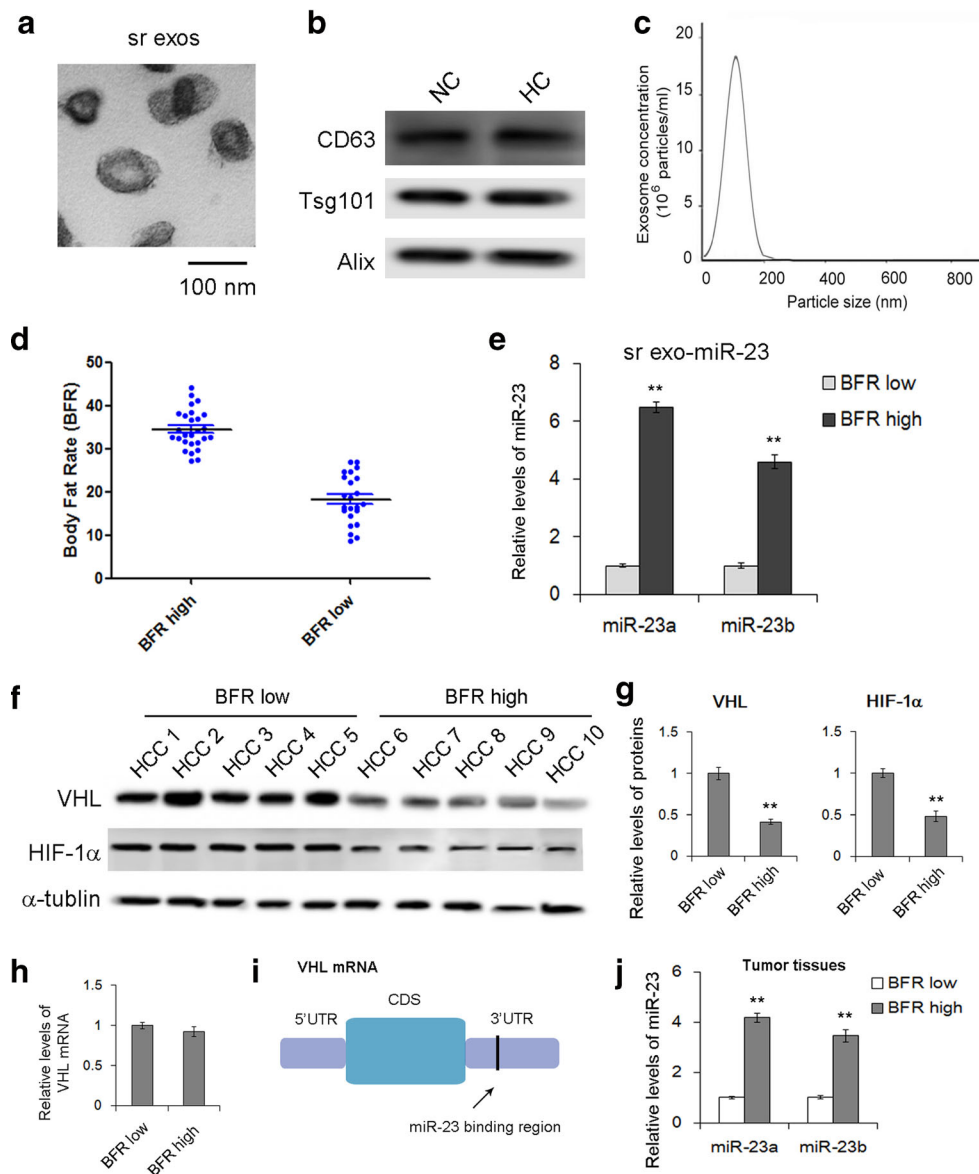


**Fig. 1** Serum exosomes from BFR-high HCC patients have higher miR23a/b copy number. **a** Electron micrograph showing exosomes isolated from human serum. Scale bar, 100 nm. **b** Exosomes were isolated from serum of healthy donors (NC), HCC patients; CD63, Tsg101, and Alix were used as the internal control of exosomes. **c** Nanoparticle tracking analysis (NTA) of isolated exosomes. **d** BFR value between HCC patients with high BFR and low BFR. **e** MiR-23a and miR-23b expression in serum exosomes from HCC patients with low

and high BFR. **f, g** Western blotting analysis of VHL and HIF-1 $\alpha$  in tumor tissues from HCC patients with low and high BFR ( $n = 5$ ): **f** Representative images, **g** quantitative analysis. **h** Quantitative RT-PCR analysis of VHL mRNA levels in tumor tissues from HCC patients with low and high BFR. **i** The binding sites of miR-23a/b in the 3'-UTR of VHL mRNA. **j** Quantitative RT-PCR analysis of miR-23a and miR-23b levels in tumor tissues from HCC patients with low and high BFR. The data represent the mean  $\pm$  s.e.m.  $^{**}P < 0.01$  (Student's  $t$  test)

mRNA level has no significant difference between two groups, indicating that VHL is regulated at the post-transcriptional level (Fig. 1h). Therefore, we use the bioinformatics method to predict the upstream factor of VHL, and found the direct interaction between miR-23a/b and the target sites in the VHL 3'-UTR (Fig. 1i). Further analysis also showed that miR23a/b was expressed with higher levels in the BFR-high group compared with the BFR-low group (Fig. 1j). Thus, miR-23a/b was higher in both BFR-high HCC serum exosomes and HCC tissues. As the target gene of miR-23a/b, VHL was expressed lower in HCC tissues with high BFR.

### The upregulation of miR-23a/b and the downregulation of VHL are related to high-BFR

A total of 698 cases were selected for further analysis, and a clear positive correlation was found between VHL levels and survival time (Fig. 2a), while a significant negative correlation was found between HIF-1 $\alpha$  levels and survival time (Fig. 2b). Obesity has been demonstrated to be closely related to HCC; thus, immunohistochemistry was performed to evaluate the VHL expression patterns in both the BFR-high group and BFR-low group. And the data showed higher VHL expression in the BFR-low group, compared with the BFR-high group (Fig. 2c).

Furthermore, we found that miR-23a/b was positively correlated with BFR (Fig. 2d and e), while VHL was negatively related to BFR in HCC (Fig. 2f). The results suggested that the new axis of miR-23/VHL/HIF-1 $\alpha$  may play a key role in obesity-mediated HCC development.

### Exo-miR-23a/b promotes proliferation of HCC cells through targeting the VHL-HIF-1 $\alpha$ pathway

Subsequently, we checked whether exo-miR-23a/b expression levels are altered during adipocyte differentiation. Pre-adipocytes were induced and differentiated into mature adipocytes, and were characterized by Oil Red O staining (Fig. 3a). Then, we isolated the exosomes from the cultured media of mature adipocytes. The isolated particles displayed the typical morphology and size of exosomes and contained TSG101, CD9, and CD63, the typical hallmarks of exosomes (Fig. 3 b and c). Quantitative reverse transcriptase-PCR (qRT-PCR) analysis was used to quantify the expression levels of miR-23a/b, in which miR-23a/b levels in the exosomes of mature adipocytes were higher than those of pre-adipocytes (Fig. 3d). Furthermore, we constructed a co-culture model to determine whether exosomes could mediate miR23a/b transferred from mature adipocytes to HCC cells (Fig. 3e). Western blotting analyses showed that 3T3 exosomes

significantly suppress VHL expression, whereas they promote the expression of HIF-1 $\alpha$ , GLUT-1, and VEGF; however, the effect of 3T3 exosomes was blocked when miR-23a, miR-23b, or miR-23a/b was removed from exosomes (Fig. 3f and g). Moreover, we performed CCK-8 to explore the effect of 3T3 exosomes on hepatocellular cancer BEL-7402 cell proliferation. BEL-7402 cells co-cultured with 3T3 exosomes exhibited increased proliferation (Fig. 3h); in contrast, the reduction of miR-23a/b in 3T3 exosomes significantly inhibited cell proliferation. Taken together, mature adipocytes secreted exosomes, which transferred miR-23a/b to HCC cells, to inhibit VHL expression level and promote tumor cell proliferation.

### VHL is a direct downstream target of miR-23a/b in HCC cells

To investigate whether VHL was inversely associated with miR-23a/b, we modulated miR-23a/b levels in HCC cell lines. Firstly, we efficiently upregulated or downregulated the miR-23a/b level in BEL-7402 cells with miR-23a/b mimics or inhibitors, respectively (Fig. 4a). Secondly, we detected the match between the miR-23a/b sequences and the full length of VHL, which showed that a VHL coding sequence (5'-AAAUAAGUUUUGCUAAAUGUGAG-3') that had a significant homology among multiple species was a potential target for miR23a/b (Fig. 4b). Subsequently, the potential miR23a/b binding sequence from VHL was cloned into the luciferase vector and co-transfected into BEL-7402 cells with miR-23a mimics, miR-23a inhibitors, or scrambled negative control RNAs. It was shown that the overexpression of miR-23a could result in a significant reduction of luciferase reporter activity compared with cells transfected with the control mimic, whereas miR-23a inhibition could result in a significant increase in reporter activity compared with cells transfected with the control inhibitor (Fig. 4c). Similar results were obtained when miR-23b was transfected instead (Fig. 4d). Next, we detected protein level by western blot. As anticipated, VHL protein level was dramatically declined, while HIF-1 $\alpha$ , GLUT-1, and VEGF protein levels were increased upon miR-23a/b overexpression, whereas treatment with the miR-23a/b inhibitor increased the levels of VHL but decreased HIF-1 $\alpha$ , GLUT-1, and VEGF protein levels (Fig. 4e and f). However, VHL mRNA level was not affected by the alteration of miR-23a/b (Fig. 4g). Thus, VHL is a direct target of miR-23a/b.

### Exo-miR-23a/b derived from adipocytes promotes chemoresistance of HCC cells

To determine whether exo-miR-23a/b confers chemoresistance in hepatocellular cancer cells, we isolated exosomes from 3T3 cells. The cells co-cultured with 3T3 cells

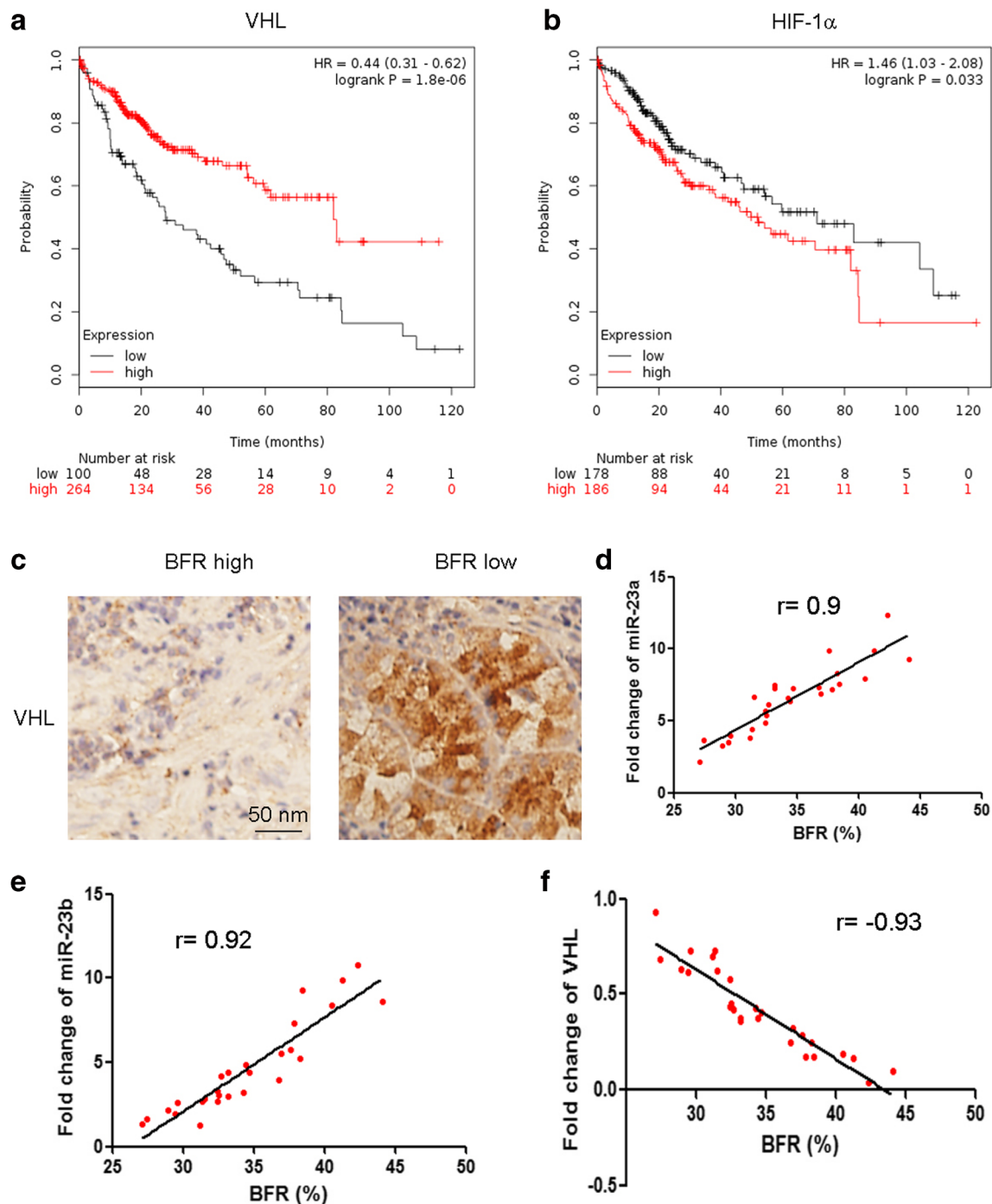


**Fig. 2** Upregulation of miR-23a/b and downregulation of VHL are related to high-BFR. **a** Increased VHL expression is associated with a better 5-year survival in HCC patients ( $n = 698$ ). **b** Increased HIF-1 $\alpha$  expression is associated with a worse 5-year survival in HCC patients ( $n = 698$ ). **c** Immunohistochemistry (IHC) analysis of VHL in HCC

patients with BFR-high and BFR-low. **d** Pearson's correlation scatter plot of the fold changes in miR-23a and BFR rates in human HCC tissue pairs. **e** Pearson's correlation scatter plot of the fold changes in miR-23b and BFR rates in human HCC tissue pairs. **f** Pearson's correlation scatter plot of the fold changes in VHL and BFR rates in human HCC tissue pairs

exosomes showed significantly lower chemosensitivity than did the PBS group. Moreover, obvious chemoresistance to 5-Fu was observed in the 3T3 exosomes with a low level of miR-23a/b compared with the 3T3 exosomes (Fig. 5a and b).

It was also shown that migration of HCC cell lines was significantly increased when cultured with 3T3 exosomes compared with PBS; the effects of exosomes could be blocked with the removal of miR-23a/b from exosomes

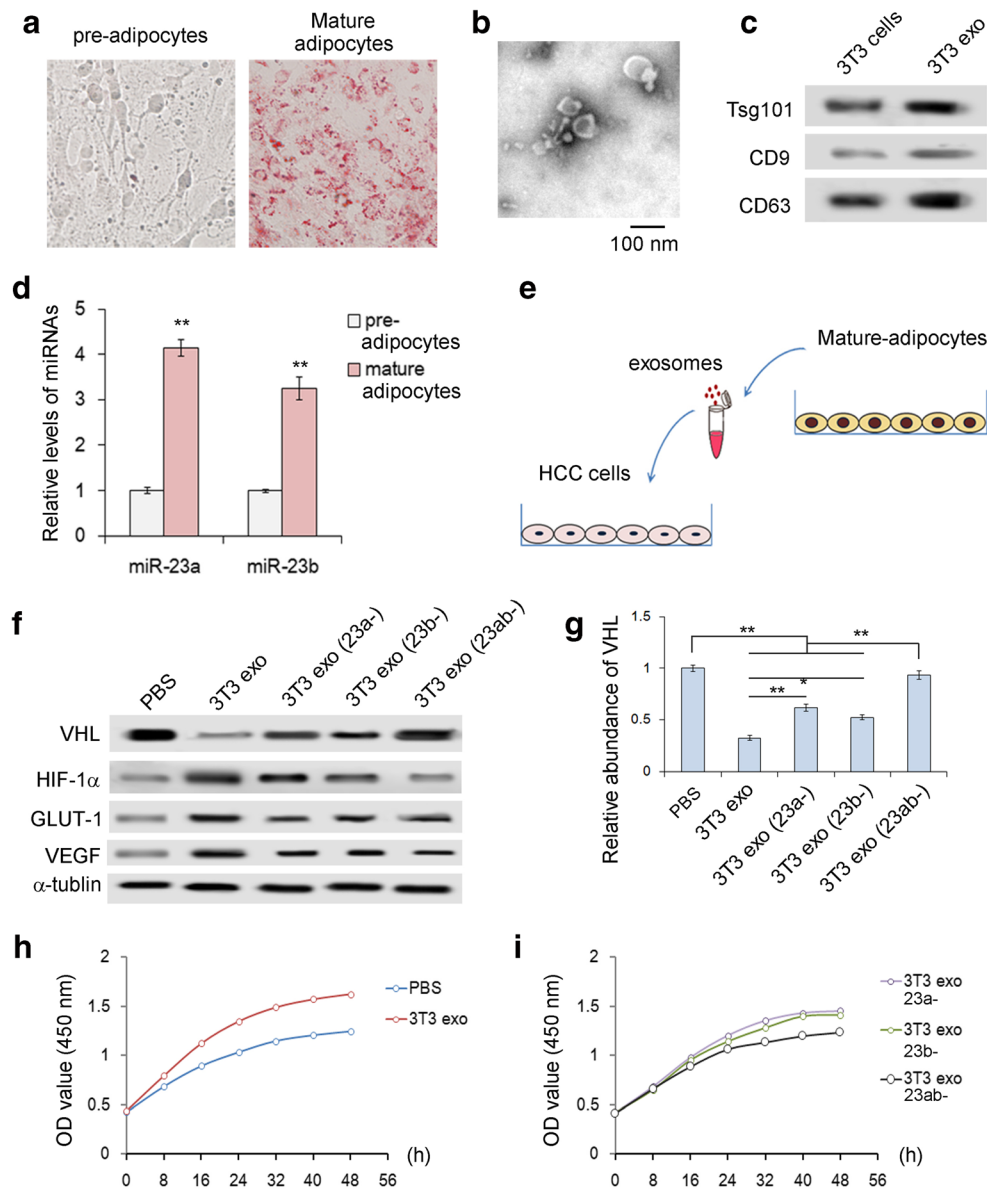


**Fig. 3** Exo-miR-23a/b promote hepatocellular cells proliferation through VHL-HIF-1 $\alpha$  pathway. **a** Pre-adipocytes cultured in standard medium; Oil Red O staining of differentiating 3T3-L1 adipocytes. **b** Electron micrograph showing exosomes isolated from the medium of 3T3 cells. Scale bar, 100 nm. **c** Tsg101, CD9, and CD63 expression in both 3T3 exosomes and 3T3 cells. **d** Quantitative RT-PCR analysis of miR-23a and miR-23b levels in pre-adipocytes and mature adipocytes. **e** Schematic

description of the experimental design: exosomes isolated from the mature adipocytes were used to culture with HCC cells. **f**, **g** Effects of 3T3 exosomes delivered miR-23a/b on VHL, HIF-1 $\alpha$ , GLUT-1, and VEGF protein levels: **f** representative images, **g** quantitative analysis. **h** 3T3 exosomes promote growth of BEL-7402 cells. **i** Effects of 3T3 exosomes delivered miR-23a/b on growth of BEL-7402 cells. The data represent the mean  $\pm$  s.e.m. \*\* $P < 0.01$  (Student's *t* test)

(Fig. 5c and d). Furthermore, Edu assay was performed to investigate the effect of exo-miR-23a/b on HCC cells' proliferation potential. The results showed that 3T3-exo promoted BEL-7402 proliferation, which could be rescued by downregulation of miR-23a/b expression level in 3T3 exosomes (Fig. 5e and f). These results firmly validated the role of miR-23a/b in promoting HCC tumorigenesis.

### Exo-miR-23a/b promotes HCC growth by targeting VHL in vivo

To further evaluate the therapeutic potential of miR-23a/b in vivo, a flowchart is shown in Fig. 6a. Both BFR ratio and body weight were elevated in the high fat diet group compared with the standard diet group (Fig. 6b and c). Exosomes in serum collected from mice were characterized by electron

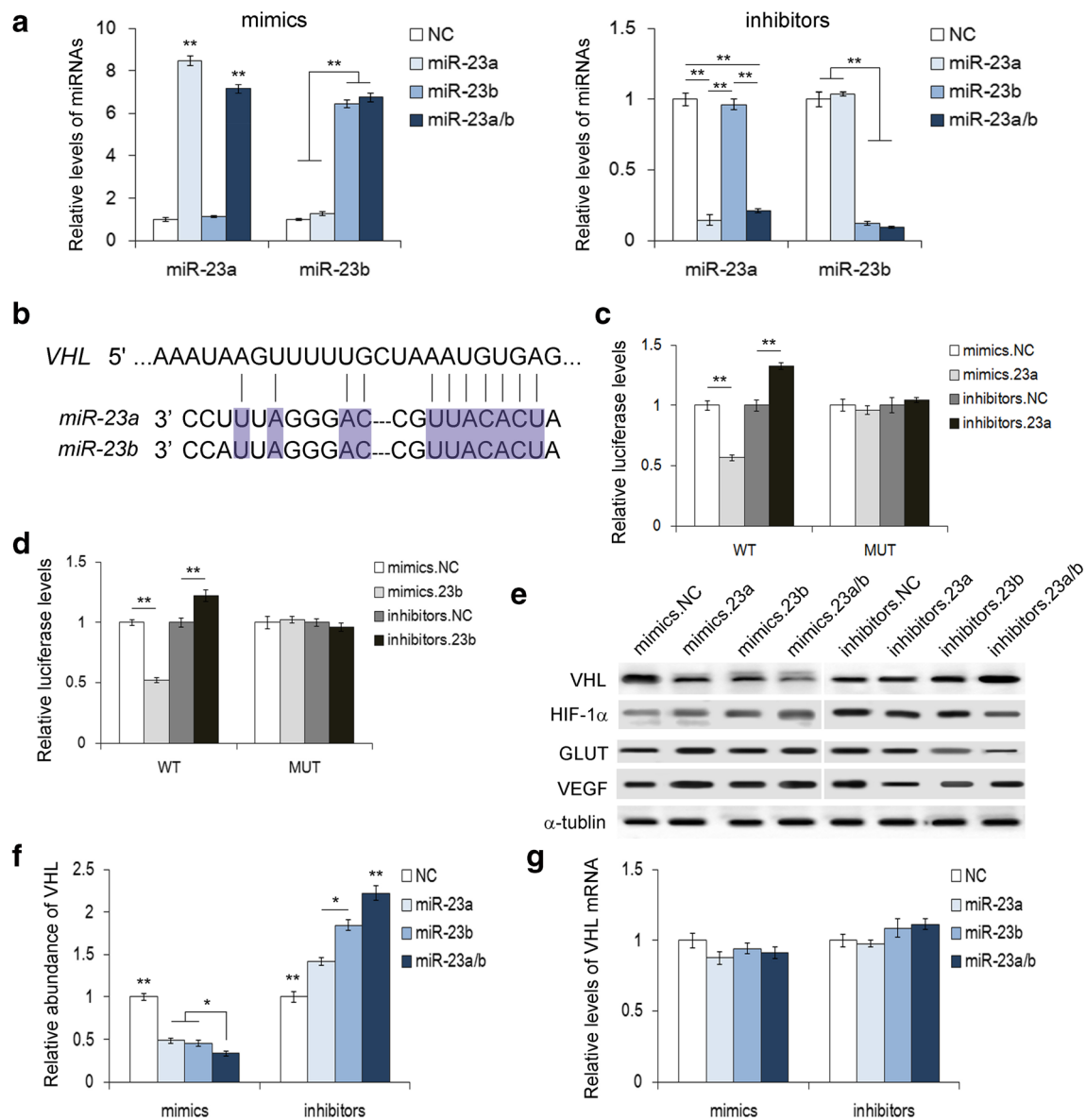


**Fig. 4** VHL is a direct downstream target of miR23a/b in HCC cells. **a** Quantitative RT-PCR analysis of miR-23a and miR-23b levels in BEL-7402 cells transfected with control mimic, miR-23a and miR-23b mimic, control inhibitor, or miR-23a and 23b inhibitor. **b** Predicted binding sites of miR-23a/b within the 3'-UTR of VHL mRNA. **c** The relative luciferase activities in BEL-7402 transfected with wild-type or mutant VHL 3'-UTR with miR-23a mimics, inhibitors, and the corresponding normal control ( $n = 3$ ). **d** The relative luciferase activities in BEL-7402 transfected with

wild-type or mutant VHL 3'-UTR with miR-23b mimics, inhibitors, and the corresponding normal control ( $n = 3$ ). **e**, **f** Western blot analysis of VHL, HIF-1 $\alpha$ , GLUT-1, and VEGF protein levels in BEL-7402 with the overexpression or suppression of miR-23a or miR-23b or miR-23a/b ( $n = 3$ ); **e** representative images, **f** quantitative analysis. **g** Relative levels of VHL mRNA in BEL-7402 transfected with miR-23a/b mimics or inhibitors ( $n = 3$ ). The data represent the mean  $\pm$  s.e.m. \* $P < 0.05$ , \*\* $P < 0.01$  (Student's  $t$  test)

microscopy and western blot analysis (Fig. 6d and e). Interestingly, reduction of miR-23a/b reversed the elevation in the BFR high group (Fig. 6f). The reduction of miR-23a/b attenuated the growth-promoting effects of obesity, indicating miR-23a/b promote tumor growth (Fig. 6h and i). Furthermore, VHL was significantly reduced, but levels of HIF-1 $\alpha$ , GLUT-1, and VEGF were increased in the tumors of the BFR high group (Fig. 6j). Therefore, these data

suggested that miR-23a/b mediated the progression of HCC with the treatment of high-fat diet (HFD).

## Discussion

Since adipose tissue is the principal source of circulating miRNAs, the serum exosomal miRNAs secreted from fat

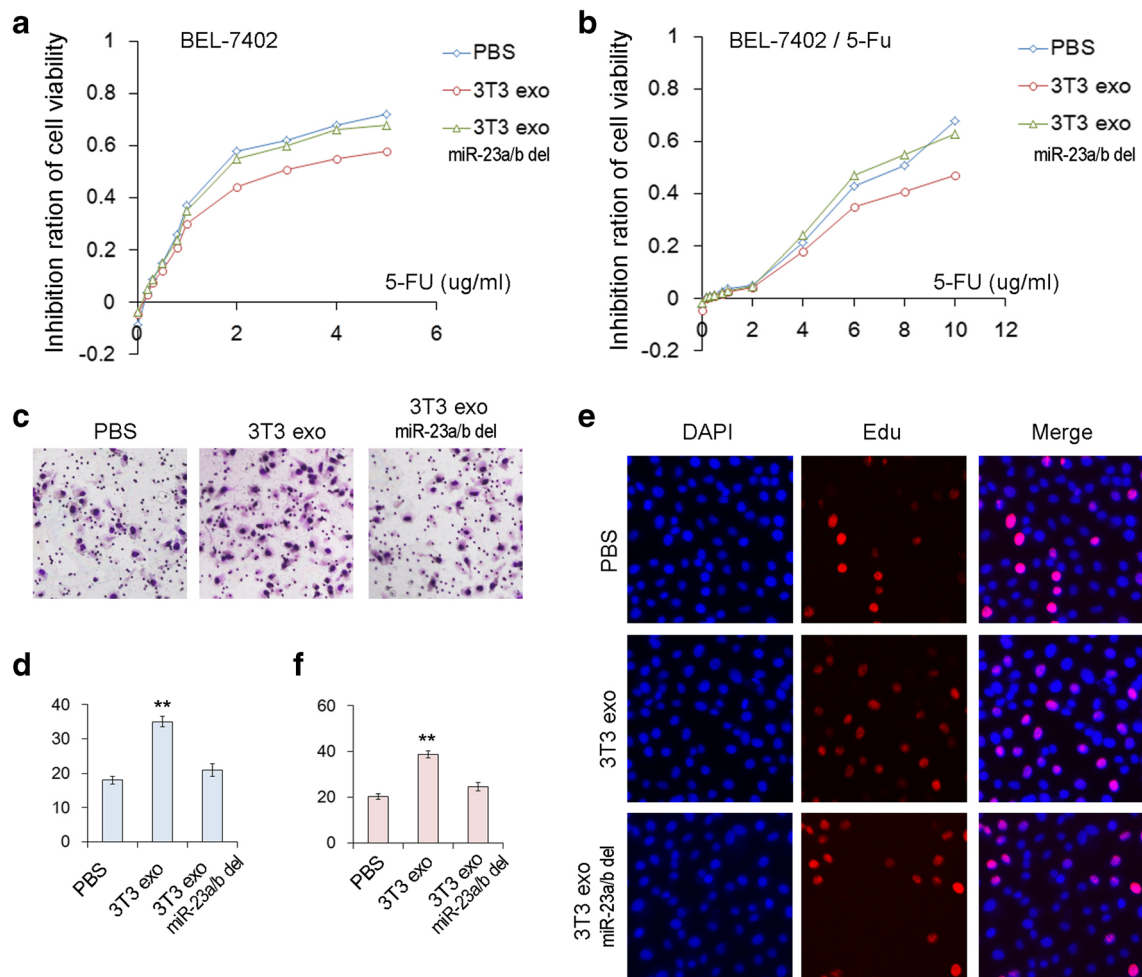


**Fig. 5** VHL is a direct downstream target of miR-23a/b in HCC cells. **a** Effects of 3T3 exosomes delivered miR-23a/b on 5-Fu sensitivity in BEL-7402 cells. **b** Effects of 3T3 exosomes delivered miR-23a/b on 5-Fu sensitivity in BEL-7402/5-Fu cells. **c, d** Upregulated miR-23a/b

promotes migration of BEL-7402 cells ( $n=3$ ): **c** representative images, **d** quantitative analysis. **e, f** Upregulated miR-23a/b promotes growth of BEL-7402 cells ( $n=3$ ): **e** representative images, **f** quantitative analysis. The data represent the mean  $\pm$  s.e.m. \*\* $P < 0.01$  (Student's  $t$  test)

may act as regulators of whole-body metabolism and the translation of mRNA in other tissues [15]. Here, we identified significantly higher expression levels of exosomes miR23a/b isolated from serum from high-BFR HCC patients than from low-BFR HCC patients. Through incubating hepatocellular cancer cells with exosomes derived from adipocytes, we confirmed that miR23a/b were successfully transferred into the HCC cells.

In this study, we use in vitro studies to show that adipocytes abundantly expressed high levels of miR23a/b, and that the exosomes mediated the transfer of miR23a/b from adipocytes to adjacent cancer cells, which could increase the chemoresistance of these recipient cells to 5-Fu and promote tumor cell migration. Therefore, our results indicated the vital role of high BFR-related exosome miR-23a/b in HCC progression.

Although we have provided evidence for the strong correlation between exosomal miR-23a/b with body fat

composition, there is no direct evidence supporting miR-23a/b in circulating exosomes in high BFR patients from adipocytes. Future studies will check whether the increased miR-23a/b is due to an indirect effect of increased BFR on other types of tissues.

It has been reported that VHL mutation is associated with several types of tumors like pheochromocytoma, clear cell renal cancer, central nervous system, and retinal angiomas, which suggests that the VHL gene may play a role as a tumor suppressor [6]. Via activation of HIF-1 $\alpha$  and HIF-2 $\alpha$ , VHL mediated adaptive responses to hypoxia. What is more, VHL could participate in extracellular matrix assembly, ciliogenesis, microtubule stabilization, senescence, and DNA repair [14]. Thus, downregulation of VHL may increase chemoresistance and tumorigenesis in renal cell cancer [18]. We showed, for the first time, that overexpression of miR-23a/b reduced the expression level of both VHL and upregulated its downstream

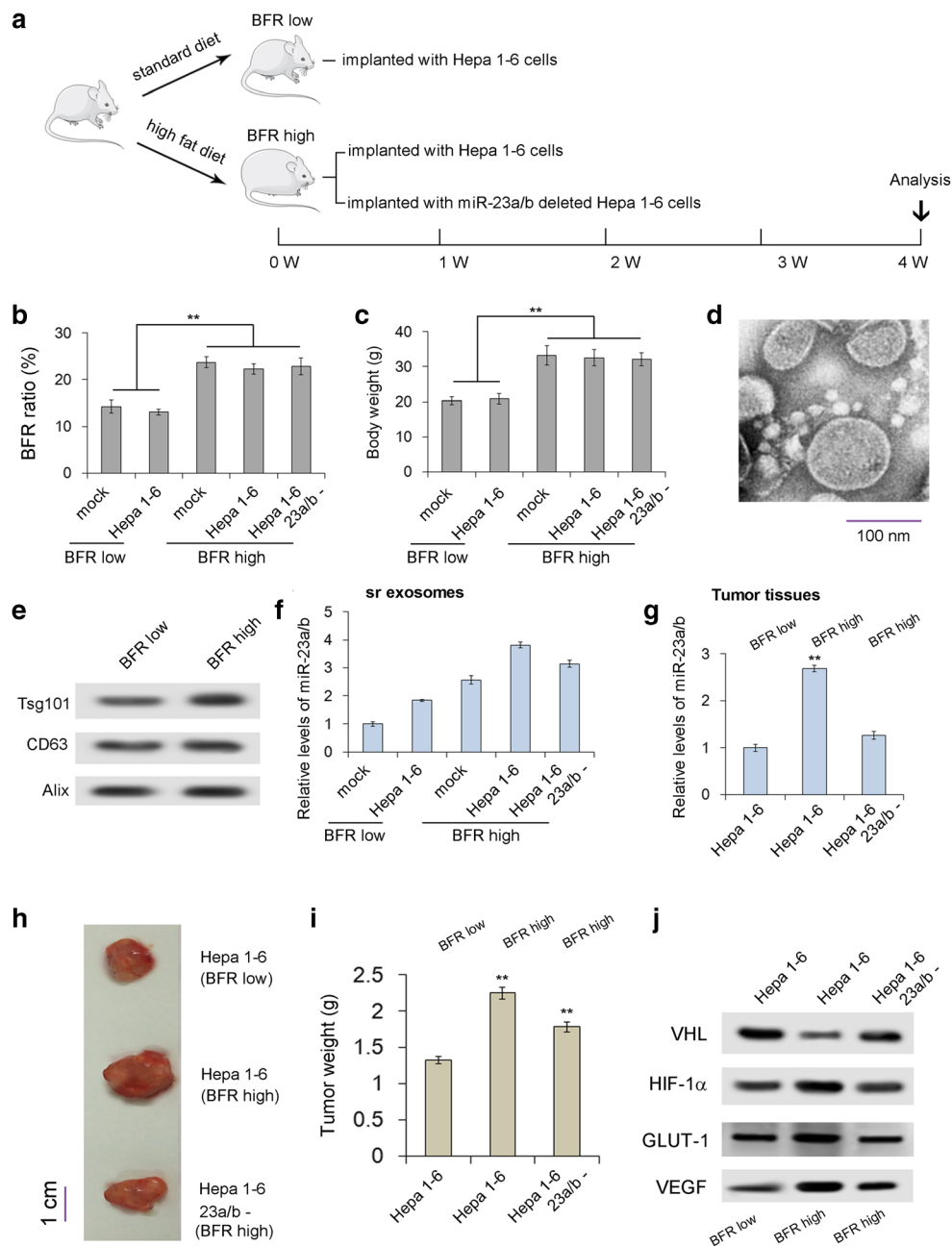


**Fig. 6** Exo-miR-23a/b promotes HCC growth in vivo by targeting VHL. **a** The C57BL/6 mice were pre-treated with standard diet or high-fat diet to obtain BFR low or BFR high model, followed by orthotopic tumor implantation; finally, mice were killed and data were analyzed on the 28th day. **a** A flow chart depicting the in vivo experimental design. **b** BFR ratio between BFR-high and BFR-low groups. **c** Body weight between BFR high and BFR low group. **d** Electron micrograph showing exosomes isolated from mouse serum. **e** Exosomes were

isolated from serum of BFR-high and BFR-low mice; Tsg101, CD63, and Alix were used as the internal control of exosomes. **f** Quantitative RT-PCR analysis of miR-23a/b levels in serum exosomes. **g** Quantitative RT-PCR analysis of miR-23a/b levels in tumor tissues from HCC mouse models. **h** Representative images of tumors from the implanted mice. **i** Quantitative analysis of xenografted tumor weight. **j** Western blot analysis of VHL, HIF-1α, GLUT-1, and VEGF protein levels in xenografted tumor. \*\* $P < 0.01$  (Student's *t* test)

targets, including HIF-1α, GLUT-1, and VEGF. Further studies suggested that miR23a/b directly binds to the VHL 3'-UTR to control the translation of VHL mRNA, and that VHL is a direct target of miR23a/b.

In conclusion, our results indicated that exo-miR23a/b derived from adipocytes can result in chemoresistance and an aggressive phenotype in HCC cells, suggesting that preventing the exosomal transfer of miR23a/b from

stromal cells may be a new strategy for suppressing HCC progression.

**Funding information** This study was supported by the Hunan Natural Science Youth Fund Project (Project number: 2018JJ3784. Project name: Molecular mechanism of miR-1181 involvement in promoting proliferation and survival of hepatocellular)

### Compliance with ethical standards

**Conflicts of interest** The authors declare that they have no conflict of interest.

**Research involving human participants and/or animals** All applicable international, national, and institutional guidelines for the care and use of animals were followed. All procedures performed in studies involving human participants were in accordance with the ethical standards of the institutional research committee and with the 1964 Helsinki declaration and its later amendments or comparable ethical standards.

**Informed consent** Informed consent was obtained from all individual participants included in the study.

### References

- An Y, Zhang Z, Shang Y, Jiang X, Dong J, Yu P, Nie Y, Zhao Q (2015) miR-23b-3p regulates the chemoresistance of gastric cancer cells by targeting ATG12 and HMGB2. *Cell Death Dis* 6:e1766
- Dyson J, Jaques B, Chattopadhyay D, Lochan R, Graham J, Das D, Aslam T, Patanwala I, Gaggar S, Cole M, Sumpter K, Stewart S, Rose J, Hudson M, Manas D, Reeves HL (2014) Hepatocellular cancer: the impact of obesity, type 2 diabetes and a multidisciplinary team. *J Hepatol* 60:110–117
- Fleshner M, Crane CR (2017) Exosomes, DAMPs and miRNA: features of stress physiology and immune homeostasis. *Trends Immunol* 38:768–776
- Gao P, Tchemyshyov I, Chang TC, Lee YS, Kita K, Ochi T, Zeller KI, De Marzo AM, Van Eyk JE, Mendell JT, Dang CV (2009) c-Myc suppression of miR-23a/b enhances mitochondrial glutamine expression and glutamine metabolism. *Nature* 458:762–765
- Gnarra JR, Tory K, Weng Y, Schmidt L, Wei MH, Li H, Latif F, Liu S, Chen F, Duh FM, Lubensky I, Duan DR, Florence C, Pozzatti R, Walther MM, Bander NH, Grossman HB, Brauch H, Pomer S, Brooks JD, Isaacs WB, Lerman MI, Zbar B, Linehan WM (1994) Mutations of the VHL tumour suppressor gene in renal carcinoma. *Nat Genet* 7:85–90
- Kuzmin I, Duh FM, Latif F, Geil L, Zbar B, Lerman MI (1995) Identification of the promoter of the human von Hippel-Lindau disease tumor suppressor gene. *Oncogene* 10:2185–2194
- Latif F, Tory K, Gnarra J, Yao M, Duh FM, Orcutt ML, Stackhouse T, Kuzmin I, Modi W, Geil L, (1993) Identification of the von Hippel-Lindau disease tumor suppressor gene. *Science* 260:1317–1320
- Liu SJ, Wang JY, Peng SH, Li T, Ning XH, Hong BA, Liu JY, Wu PJ, Zhou BW, Zhou JC, Qi NN, Peng X, Zhang JF, Ma KF, Cai L, Gong K (2018) Genotype and phenotype correlation in von Hippel-Lindau disease based on alteration of the HIF- $\alpha$  binding site in VHL protein. *Genet Med* 20:1266–1273
- Najafi Z, Sharifi M, Javadi G (2019) LNA inhibitor in microRNA miR-23b as a potential anti-proliferative option in human hepatocellular carcinoma. *J Gastrointest Cancer*. <https://doi.org/10.1007/s12029-019-00215-y>
- Ray K (2013) Gut microbiota: obesity-induced microbial metabolite promotes HCC. *Nat Rev Gastroenterol Hepatol* 10:442
- Semenza GL (1999) Regulation of mammalian O<sub>2</sub> homeostasis by hypoxia-inducible factor 1. *Annu Rev Cell Dev Biol* 15:551–578
- Sruthi TV, Edatt L, Raji GR, Kunhiraman H, Shankar SS, Shankar V, Ramachandran V, Poyyakkara A, Kumar SVB (2018) Horizontal transfer of miR-23a from hypoxic tumor cell colonies can induce angiogenesis. *J Cell Physiol* 233:3498–3514
- Sun Z, Shi K, Yang S, Liu J, Zhou Q, Wang G, Song J, Li Z, Zhang Z, Yuan W (2018) Effect of exosomal miRNA on cancer biology and clinical applications. *Mol Cancer* 17:147
- Tarade D, Ohh M (2018) The HIF and other quandaries in VHL disease. *Oncogene* 37:139–147
- Thomou T, Mori MA, Dreyfuss JM, Konishi M, Sakaguchi M, Wolfrum C, Rao TN, Winnay JN, Garcia-Martin R, Grinspoon SK, Gorden P, Kahn CR (2017) Adipose-derived circulating miRNAs regulate gene expression in other tissues. *Nature* 542:450–455
- Wendler F, Favicchio R, Simon T, Alifrangis C, Stebbing J, Giamas G (2017) Extracellular vesicles swarm the cancer microenvironment: from tumor-stroma communication to drug intervention. *Oncogene* 36:877–884
- Yu J, Shen J, Sun TT, Zhang X, Wong N (2013) Obesity, insulin resistance, NASH and hepatocellular carcinoma. *Semin Cancer Biol* 23:483–491
- Yuen JS, Cockman ME, Sullivan M, Protheroe A, Turner GD, Roberts IS, Pugh CW, Werner H, Macaulay VM (2007) The VHL tumor suppressor inhibits expression of the IGF1R and its loss induces IGF1R upregulation in human clear cell renal carcinoma. *Oncogene* 26:6499–6508
- Zatyka M, da Silva NF, Clifford SC, Morris MR, Wiesener MS, Eckardt KU, Houlston RS, Richards FM, Latif F, Maher ER (2002) Identification of cyclin D1 and other novel targets for the von Hippel-Lindau tumor suppressor gene by expression array analysis and investigation of cyclin D1 genotype as a modifier in von Hippel-Lindau disease. *Cancer Res* 62:3803–3811
- Zhang H, Deng T, Liu R, Bai M, Zhou L, Wang X, Li S, Yang H, Li J, Ning T, Huang D, Li H, Zhang L, Ying G, Ba Y (2017) Exosome-delivered EGFR regulates liver microenvironment to promote gastric cancer liver metastasis. *Nat Commun* 8:15016

**Publisher's note** Springer Nature remains neutral with regard to jurisdictional claims in published maps and institutional affiliations.